

Fabrication and Assembly of Ultrathin Silicon Solar Microcells Integrating Electrical Passivation and Anti-reflection Coatings

Yuan Yao, Eric Brueckner, Lanfang Li, and Ralph Nuzzo

Supplementary Information

Figure S1 shows a schematic overview of the fabrication process.

Cleaning

The process started with a boron-doped Czochralski silicon wafer (“prime” grade, 3-inch diameter, (111) $\pm 0.1^\circ$ orientation, 7.5-10 $\Omega\cdot\text{cm}$, 380 μm thickness, Silicon Materials). Wafers were rinsed with acetone and isopropyl alcohol (IPA). Prior to all high temperature processes, RCA cleaning procedures were used, detailed below:

RCA1 Clean

Etch in RCA1 solution ($\text{H}_2\text{O}:\text{NH}_3\cdot\text{H}_2\text{O}:\text{H}_2\text{O}_2 = 5:1:1$) at 80°C for 10 min

RCA2 Clean

Etch in RCA1 solution ($\text{H}_2\text{O}:\text{HCl}:\text{H}_2\text{O}_2 = 5:1:1$) at 80°C for 10 min

Native oxide on the wafer was removed by buffered oxide etchant (BOE 6:1, Transene) before and after each cleaning step.

Phosphorus Doping

The cleaned wafers were first doped by solid-state sources of phosphorus (PH-1000N, Saint Gobain). Etching the phosphosilicate glass (PSG) layer in BOE 10:1 and RCA cleaning completed the doping process.

Phosphorous doping over a variety of temperatures (900°C , 950°C , and 1000°C) and times (5 min, 15 min, and 30 min) was conducted to ultimately optimize conversion

efficiency of the μ -cells. To directly compare the effect of doping time and temperature parameters, three batches of three wafers were processed simultaneously, each wafer within the batch doped for a different time (Batch 1: 1000°C, Batch 2: 950°C, Batch 3: 900°C). To eliminate possible variations in light absorption from the anti-reflective, oxide layers (the thickness of oxide on device differs from batch to batch), the μ -cells were immersed in BOE 6:1 to remove all oxide prior to testing. Figure S2 shows normalized efficiency vs. doping time for the three temperatures of interest. The doping conditions giving the highest conversion efficiency in each batch were 1000°C for 5 min, 950°C for 5 min, and 900°C for 15 min, giving sheet resistance values of 22 Ω/\square , 80 Ω/\square , and 78 Ω/\square , respectively, measured by four point probe (Pro4, Signatone). These conditions were then directly compared in a fourth batch to eliminate batch-to-batch variability. Figure S3A shows the doping profiles measured by quantitative secondary-ion mass spectrometry (SIMS) and Figure S3B shows averaged I - V curves of cells doped at 900°C, 950°C, and 1000°C for 15 min, 5 min, and 5 min, respectively. Table 1 and Figure S4 shows the parameters of J_{sc} , V_{oc} , η , and FF . The data shows that doping at 900°C for 15 min gives the highest conversion efficiency, leading us to adopt this as the standard protocol for μ -cell fabrication.

Temp (°C)	J_{sc} (mA/cm ²)	V_{oc} (V)	η (%)	FF
900 (15 min)	27.15	0.538	10.6	0.727
950 (5 min)	26.55	0.541	10.0	0.699
1000 (5 min)	23.83	0.543	9.3	0.719

Table 1

Thermal Oxidation and Photolithography

A top oxide mask layer was then grown by wet oxidation at 1000 °C for 80-100 min under steam atmosphere (<0.2 LPM O₂ flow through boiling DI water) in a quartz tube furnace following RCA1 and RCA2 cleanings outlined above. The lateral dimensions of the μ -cells were defined by standard photolithographic processing (AZ5214-E, AZ Electronic Materials):

Spin-coat hexamethyldisilazane (HMDS) at 5000 rpm for 30 sec

Spin-coat AZ5214-E at 5000 rpm for 30 sec

Softbake at 110°C for 60 sec

Expose 310 mJ/cm² at 320 nm (Karl Suss MJB3 mask aligner)

Develop in metal ion free (MIF) 327 for ~100 sec

O₂ descum (20 sccm, 250 mTorr, 50 W) for 60 sec

Hardbake at 110°C for 180 sec

The oxide not covered by the photoresist was then removed by BOE 6:1 (~12 min). Inductively coupled plasma reactive ion etching (ICP-RIE, Surface Technology Systems) was utilized to define the vertical depth of the trench structures. Standard Bosch Processing conditions were used: chamber pressure of 81.5 mTorr, etching for 7 sec/cycle with 130 sccm SF₆ and 13 sccm O₂ under 600 W coil power and 12 W platen power, then passivating for 5 sec/cycle with 110 sccm C₄F₈ under 600 W coil power and 0 W platen power. Etch times were controlled such that an etch depth of 35-40 μ m was achieved, typically 75 cycles. The remaining photoresist was then removed by sonicating in acetone and RCA1 cleaning.

Brief Undercut and Sidewall Oxidation

A short anisotropic etching step of the wafer was performed in 25 wt.% tetramethylammonium hydroxide solution (TMAH, Sigma-Aldrich) at 70°C for 2 min to achieve a canopy-type structure. The exposed sidewalls ($\{110\}$) of cells etched at ~ 1 $\mu\text{m}/\text{min}$ according to cross-sectional SEM images shown in Figure 1B. After RCA cleanings, a second wet oxidation step (1000 °C, 20-25 min) formed an oxide layer on the side and bottom of the trenches and increased the oxide thickness on top of the cells as well, shown in Figure S5A.

Flood RIE and Undercut

The oxide on the bottom of the trenches was selectively removed by reactive-ion etching (Plasma Therm 790 series) using CHF_3 (20 sccm) and O_2 (8 sccm) under 50 mtorr and 175 W for ~ 9 min. This dry etch is pseudo-anisotropic such that little oxide on the sidewall was consumed (Figure S5B). After immersion in BOE 6:1 for ~ 20 sec, the wafer was immersed into 25% TMAH solution at 80°C for ~ 90 min to fully undercut the μ -cells and release them from the substrate except at anchor locations.

Boron Doping

After RCA cleaning, the back surface field was formed by solid-source boron doping (BN-975, Saint Gobain) at 1000 °C for 30 min. The borosilicate glass (BSG) layer was etched in 20:1 HF for ~ 2 min. Oxide remaining on the top and sidewall surfaces (Figure S5C) now serves as passivation and anti-reflection layers.

Patterning Top Contacts

Square contacts (50 $\mu\text{m} \times 50 \mu\text{m}$) were defined through photolithography with a photoresist (AZ P4620, Clariant):

Spin-coat HMDS at 2000 rpm for 30 sec

Spin-coat AZ5214-E at 1000 rpm 10 sec, then at 2000 rpm for 30 sec

Softbake at 65°C for 5 min and then at 95°C for 20 min,

Expose 410 mJ/cm² at 365 nm

Develop in 3:1 AZ400K(AZ Electronic Materials) for ~1 min

Expose under UV-generated ozone for 2 min

Hardbake at 65°C for 30 min (ramp from 35°C with a ramp rate of 0.5°C/min)

The oxide not protected by the photoresist was then removed by BOE 6:1 (~5.5 min) and Ti (10 nm) /Au (300 nm) contact pads were formed by e-beam evaporation and photoresist lift-off in acetone.

Statistical Analysis of Fabricated Si Solar μ -Cells

To test the large-area reliability of the fabrication process, we transferred μ -cells from the entire patterned wafer area. Specifically, every sixth device in all six rows was picked-up with a PDMS stamp and transferred to a glass substrate (discussed subsequently) for *I-V* testing. The μ -cells were tested under simulated AM1.5D illumination of 1000 W·m⁻² at room temperature prior to planarization of the μ -cells on an anodized Al plate to minimize reflection from the back plane. Using the top surface area of the μ -cells as the device area, the PV metrics of J_{sc} , V_{oc} , η , and FF were measured and plotted with histograms shown as insets (Figure S6 and Figure 2C).

Transfer Printing μ -Cells

The receiving substrate was made by spin-coating a UV-curable polymer (NOA61, Norland Products, 3000 rpm for 45 sec) on a pre-cleaned glass slide (5 cm × 5 cm × 2 mm) and partially curing under UV light (1260 mJ/cm² at 365 nm) with a Karl Suss

MJB3 mask aligner. Bottom electrodes were then deposited by e-beam evaporation of Ti (10 nm) /Au (300 nm) through a shadow mask.

Microcells were selectively picked up by a PDMS (10:1 ratio of pre-polymer to initiator, Sylgard 184, Dow Corning) stamp with pyramidal structures and printed on the receiving substrate with an automated transfer printing machine. By applying modest pressure on the inked stamp to the receiving substrate, excellent electrical contact was achieved between the bottom electrode and device. Step and repeat printing allowed formation of arrays with arbitrary configurations. The fabrication of the pyramid PDMS stamp and the manipulation of the automated machine were described elsewhere (see Ref. 36).

After printing, the μ -cells were tested and baked at 150 °C on hotplate for 10 min. This postbake step possibly caused the partially cured NOA layer to reflow and intimately coat the bottom side of the μ -cell, preventing liquid pre-polymer to flow underneath the device and block the back contact in the following planarization step.

Planarization

A flat PDMS block (10:1 ratio of pre-polymer to initiator) was laminated on top of the printed devices to achieve conformal contact with the μ -cells. Silica particles (30 μ m diameter, SPI) were dispersed on the substrate around the device area to support the PDMS stamp and avoid sagging. Another UV-curable polymer (NOA73, Norland Products) was dispensed in a reservoir created in the PDMS block with a 3 mm biopsy punch. The liquid pre-polymer flowed by capillary action to fill the air gap between the PDMS and substrate. The entire system was then exposed under UV light to cure the NOA, before PDMS was peeled off from the substrate, leaving the μ -cells embedded in

the NOA matrix. A profilometry line scan (Figure S8A) of the resulting planarization layer shows minimal topological variation between cells ($\sim 5\ \mu\text{m}$).

Interconnection

Interconnecting the planarized μ -cells was accomplished by manually aligning a stencil mask (two pieces of Scotch® tape) to form the shape of the interconnect. A small volume ($\sim 0.5\ \text{mL}$) of Ag paste (Ted Pella, PELCO® Conductive Silver 187) was dispensed on one end, using a razor blade to “squeegee” the Ag paste over and into the stencil mask. The Scotch® tape stencil mask was peeled away immediately, leaving behind a well-formed interconnection line $\sim 150\ \mu\text{m}$ wide and $\sim 50\ \mu\text{m}$ tall (Figure S8B). The Ag paste line was cured in air at room temperature for 30 min prior to any electrical measurements.

Measurements under Concentration

To aid thermal and electrical conduction due to intense illumination and increased photocurrent generation, respectively, from concentrated solar flux, devices were assembled differently than the procedure described above. After device fabrication, the μ -cells were conformally contacted by a PDMS stamp and lifted off from the donor wafer. Thin-film metal ohmic contacts ($\sim 150\ \mu\text{m}$ wide, Ti (5 nm)/Au (200 nm)) were e-beam evaporated on the backside of the μ -cells through a shadow mask. The μ -cells were then embedded in a thin ($\sim 200\ \mu\text{m}$) line of uncured Ag epoxy (E4110, Epoxy Technology) on a glass slide. The glass slide/Ag epoxy/ μ -cell/PDMS system was baked on a 150°C hot plate for 15 min. Following the baking step, the PDMS stamp was slowly removed, leaving the μ -cells printed on a cured Ag epoxy matrix serving as the interconnection on the backside of the devices. There was not a subsequent planarization step with NOA.

During solar measurements under concentration, the glass slide was mounted on an anodized aluminum plate with a 3 inch fan used to cool the μ -cells. Concentration ratios (x) for Figures 5E and 5F were calculated by the following expression:

$$I_{\text{sc,conc}} = xI_{\text{sc,1sun}}$$

where $I_{\text{sc,conc}}$ and $I_{\text{sc,1sun}}$ is the short-circuit current for a μ -cell under concentration and 1 sun, respectively.

Solar μ -Cell Characterization

I - V characteristics of the μ -cells were measured with a source meter (Keithley, Model 2400) under a full-spectrum solar simulator (Model 91192, Oriel) with AM 1.5D filter calibrated to $1000 \text{ W}\cdot\text{cm}^{-2}$ at room temperature using a Si reference cell (Model 91150V, Newport-Oriel). Measurements under solar concentration were obtained by placing a convex lens (Model LH-2 M4 KBX145 F62.9, Newport) in the beam path. Different concentration ratios were obtained by translating the lens vertically.

Due to the inherent transparency of printed arrays of these μ -cells, reflection from the subjacent layers will have a significant impact on PV measurements. We suppressed reflection from the solar simulator's sample stage by mounting the glass substrate on an anodized Al (AA) plate to obtain PV metrics with minimal influence of reflected light. Figure S9 shows reflectivity data, relative to a Spectralon® target, of the anodized Al (AA) plate used for PV measurements. To elucidate enhancements to the PV metrics of printed μ -cells from diffuse reflection, the glass substrate was also mounted on a Spectralon® target, as shown in Figure 5A, in some measurements. We distinguish reported PV metrics when using this diffuse backside reflector by using subscript "BSR".

For devices without oxide, *I-V* characteristics were measured right after a 5.5 min etch in BOE 6:1 as well as a few days later after the formation of the native oxide layer on an AA plate without planarization. (See Figure S7A and Table2). The devices show a further degradation after the surface Si-H bonds formed during BOE etch were oxidized in air. The data with the native oxide layer is used in Figure 3A.

	J_{sc} (mA/cm ²)	V_{oc} (V)	Efficiency (%)	FF
With Oxide	28.08	0.515	10.89	0.753
After BOE	19.85	0.501	7.54	0.758
Without Oxide (With Native Oxide)	19.08	0.481	6.80	0.740

Table 2

EQE measurements were taken using an OL750 spectroradiometer with devices embedded in NOA layer with top contact lines. The top interconnects for devices in Figure 3B and Figure S7E were formed by either sputtering a Ti (10nm)/Al (300nm) metal line or directly painting a silver paste/epoxy line through a stencil mask onto the cell. All EQE results were normalized to percentage based on device performance under AM1.5D solar spectrum measured on a non-reflective AA plate without planarization to eliminate waveguiding effects.

Methods for calculating the AR effects from the top oxide

The reflections on the top surface of the device were calculated based on refractive indices of thermal oxide (n_2) and silicon (n_1) at different wavelengths (λ), assuming a normal incidence of the incoming solar radiation. (Refractive indices at different wavelength for single-crystalline silicon and fused silica were taken from

“*Handbook of Optical Constants of Solids*, Edward D. Palik. Academic Press, Boston, 1985” and “*Handbook of Optics, 3rd edition, Vol. 4. McGraw-Hill 2009*”, respectively.)

For devices without oxide, the top surface reflection (R_1) under air was calculated as

$$R_1 = \frac{(n_1 - 1)^2}{(n_1 + 1)^2}$$

For devices with oxide with a certain thickness (t), the top surface reflection (R_2) was calculated as

$$R_2 = \frac{r_1^2 + r_2^2 + 2r_1r_2 \cos 2\theta}{1 + r_1^2r_2^2 + 2r_1r_2 \cos 2\theta}$$

where

$$r_1 = \frac{1 - n_2}{1 + n_2}; r_2 = \frac{n_2 - n_1}{n_2 + n_1}; \theta = \frac{2\pi n_2 t}{\lambda}$$

The relative optical enhancement (E) by adding a thermal oxide AR layer was then defined as

$$E = \frac{1 - R_2}{1 - R_1}$$

The EQE for a device with AR coating but without passivation was then estimated as

$$EQE_{\text{simulated}} = \frac{1 - R_2}{1 - R_1} \cdot EQE_{\text{without oxide}}$$

The difference between these two EQE curves were then integrated with the AM 1.5D solar spectrum to get the simulated current density enhancement from an AR layer on a device without passivation.

For the blue dashed curve in Figure 3B, 250 nm was used as the oxide thickness for calculation, as determined by a cross-sectional SEM image (Figure S7B) for another device on the same donor wafer.

SI Figure Captions

Figure S1 Schematic illustration of the fabrication protocol for creating Si solar μ -cells.

Figure S2 Efficiency normalized to the maximum efficiency for each data series (i.e., doping temperature) vs. phosphorous doping time. The data shows that the maximum efficiency is achieved at doping times of 15 min, 5 min, and 5 min at doping temperatures of 900°C, 950°C, and 1000°C, respectively.

Figure S3 (A) SIMS depth profile of phosphorous concentration in samples doped at different conditions; (B) J - V curves of μ -cells doped at different conditions measured on an AA plate without planarization. (900°C, 15 min: black, 950°C, 5 min: red; 1000 °C, 5min: blue)

Figure S4 Performance metrics of devices doped at different conditions measured on an AA plate without planarization: (A) J_{sc} ; (B) V_{oc} ; (C) Efficiency; and (D) Fill factor.

Figure S5 Cross-sectional SEM images of Si μ -cells (blue) with thermally grown oxide layers (pink) on the top (left frame) and sidewall (right frame) surface after different fabrication steps: (A) Sidewall oxidation; (B) Flood RIE; and (C) Full device fabrication.

Figure S6 Statistical analyses and histogram plots (insets) of device performance metrics measured on an AA plate without planarization: (A) J_{sc} ; (B) V_{oc} ; and (C) Fill factor.

Figure S7 (A) J - V characteristics of devices with oxide (black), right after BOE etch (green) and after formation of a native oxide layer (red); (B) Cross-sectional SEM images of a Si μ -cell for EQE measurement with top oxide thickness of ~ 250 nm; (C) Calculated top surface reflections for devices without oxide (red) and with 250 nm thermal oxide (black); (D) Simulated relative AR enhancements for a μ -cell with 250 nm top oxide; (E) External quantum efficiencies (EQE) of passivated μ -cells with various oxide thickness.

Figure S8 (A) Profilometry line scan across three printed Si solar μ -cells following planarization; (B) Profilometry line scan across a Ag paste interconnect.

Figure S9 Reflectance of the non-reflective anodized aluminum (AA) plate.

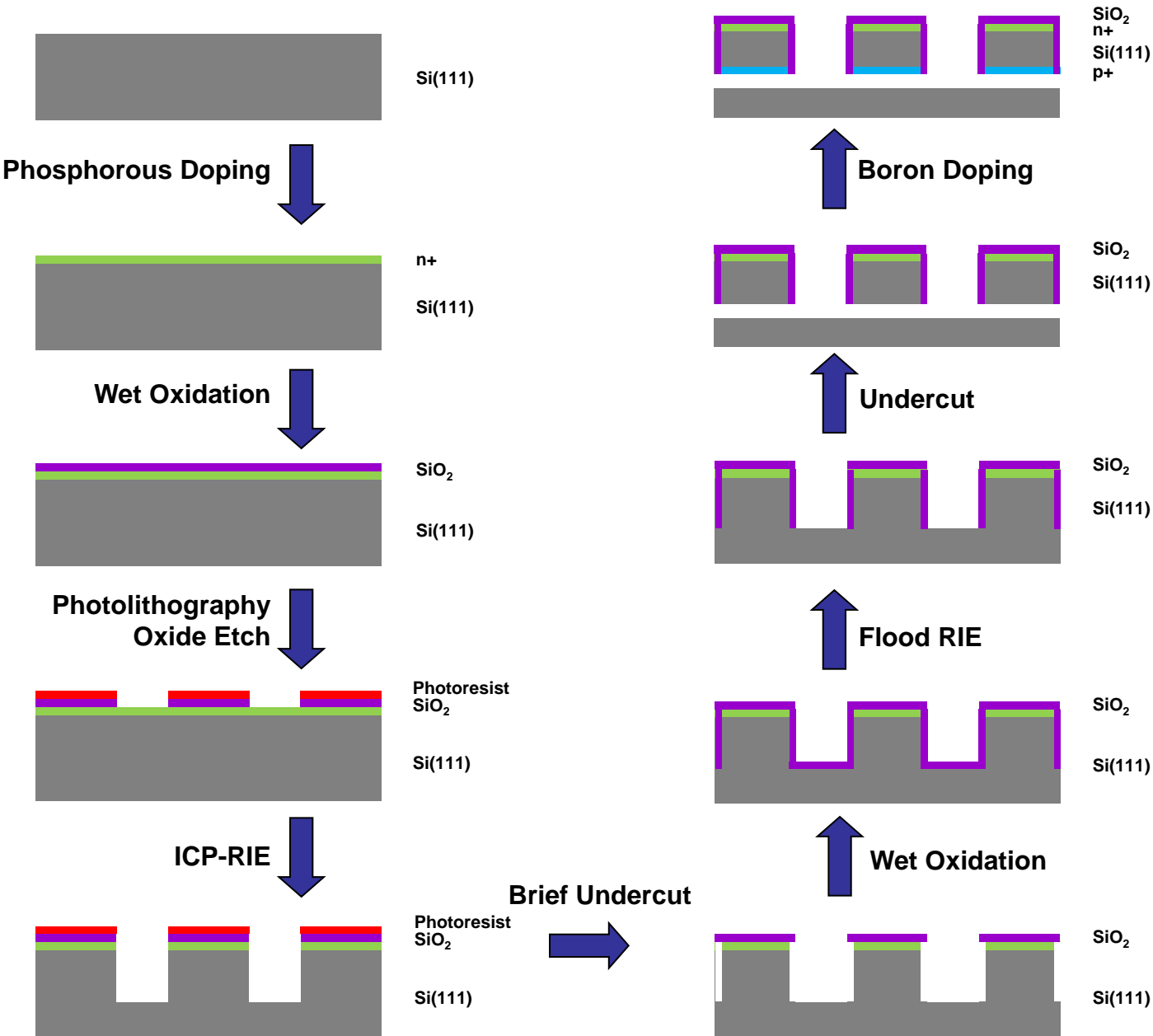


Figure S1

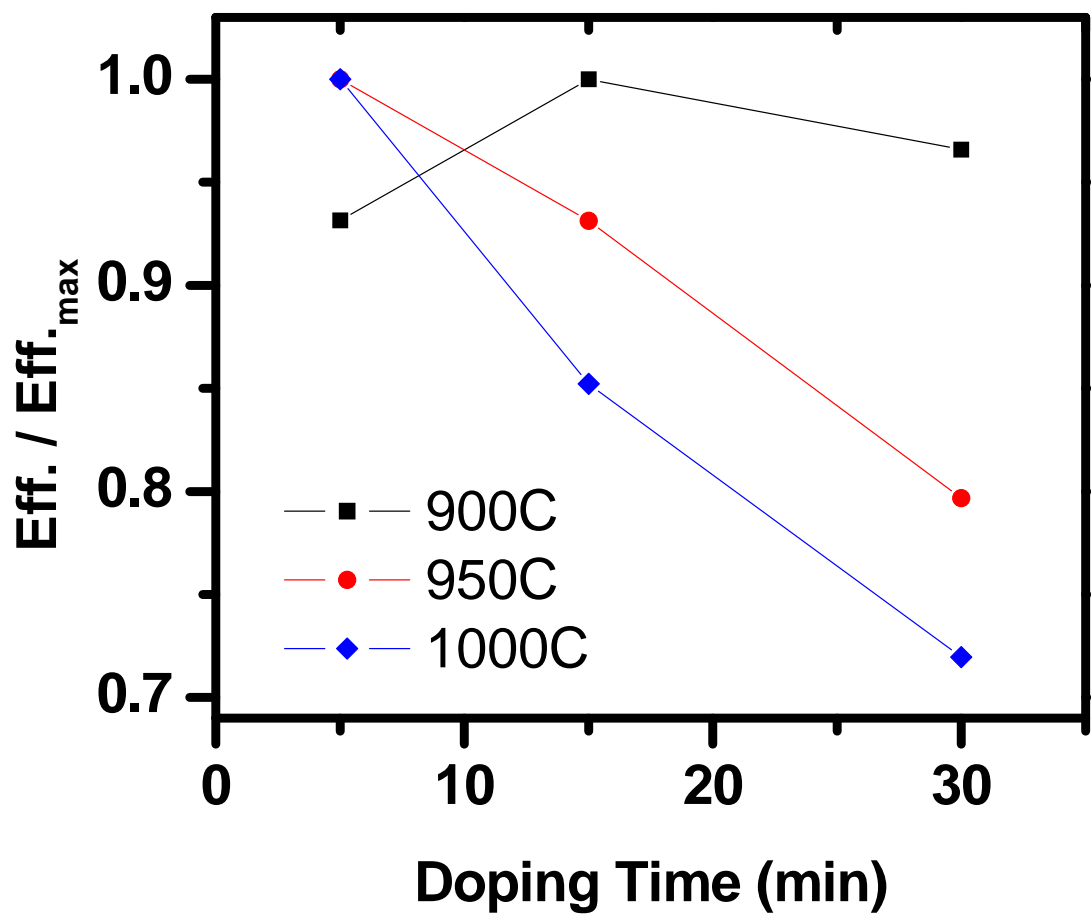


Figure S2

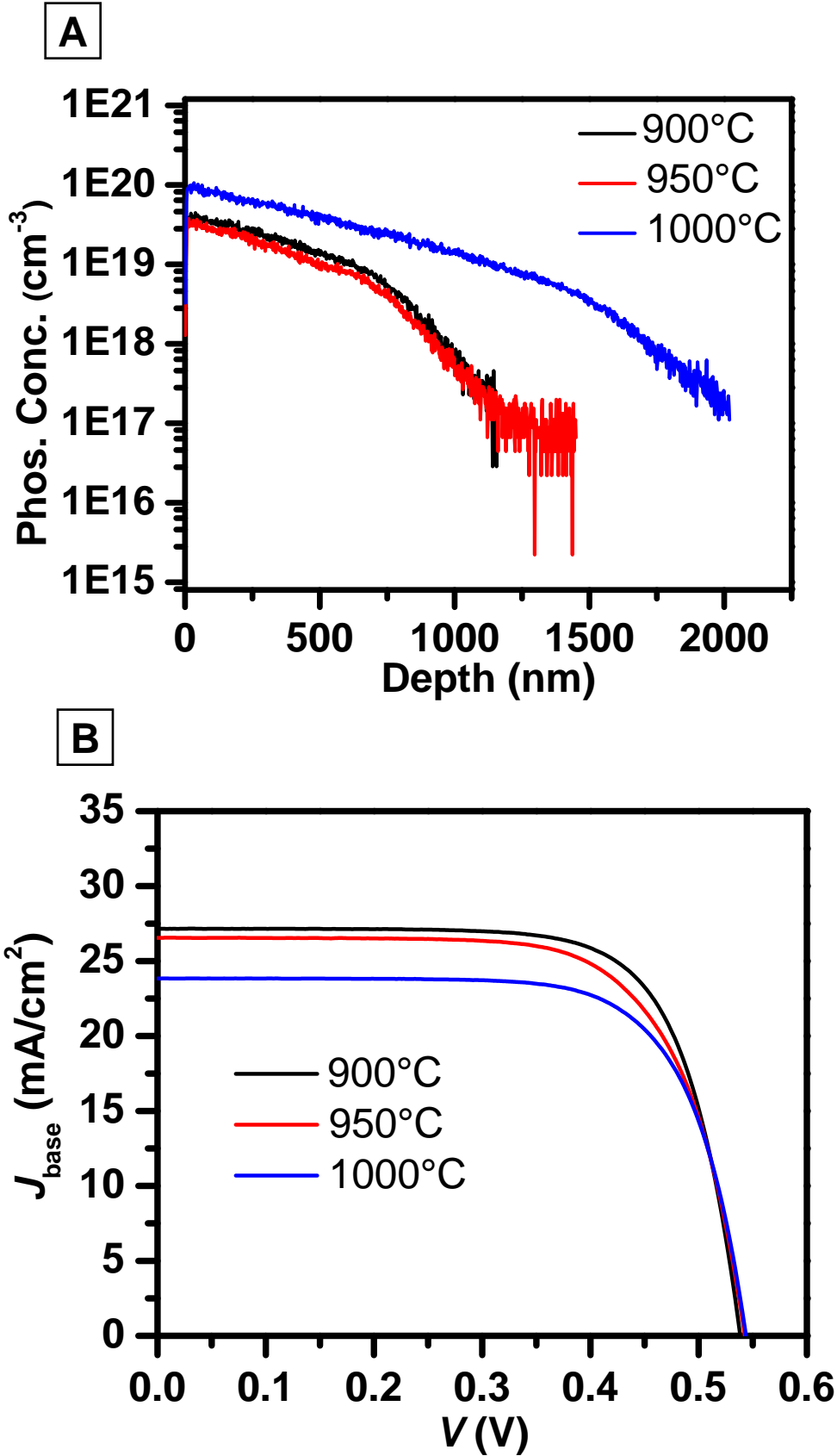


Figure S3

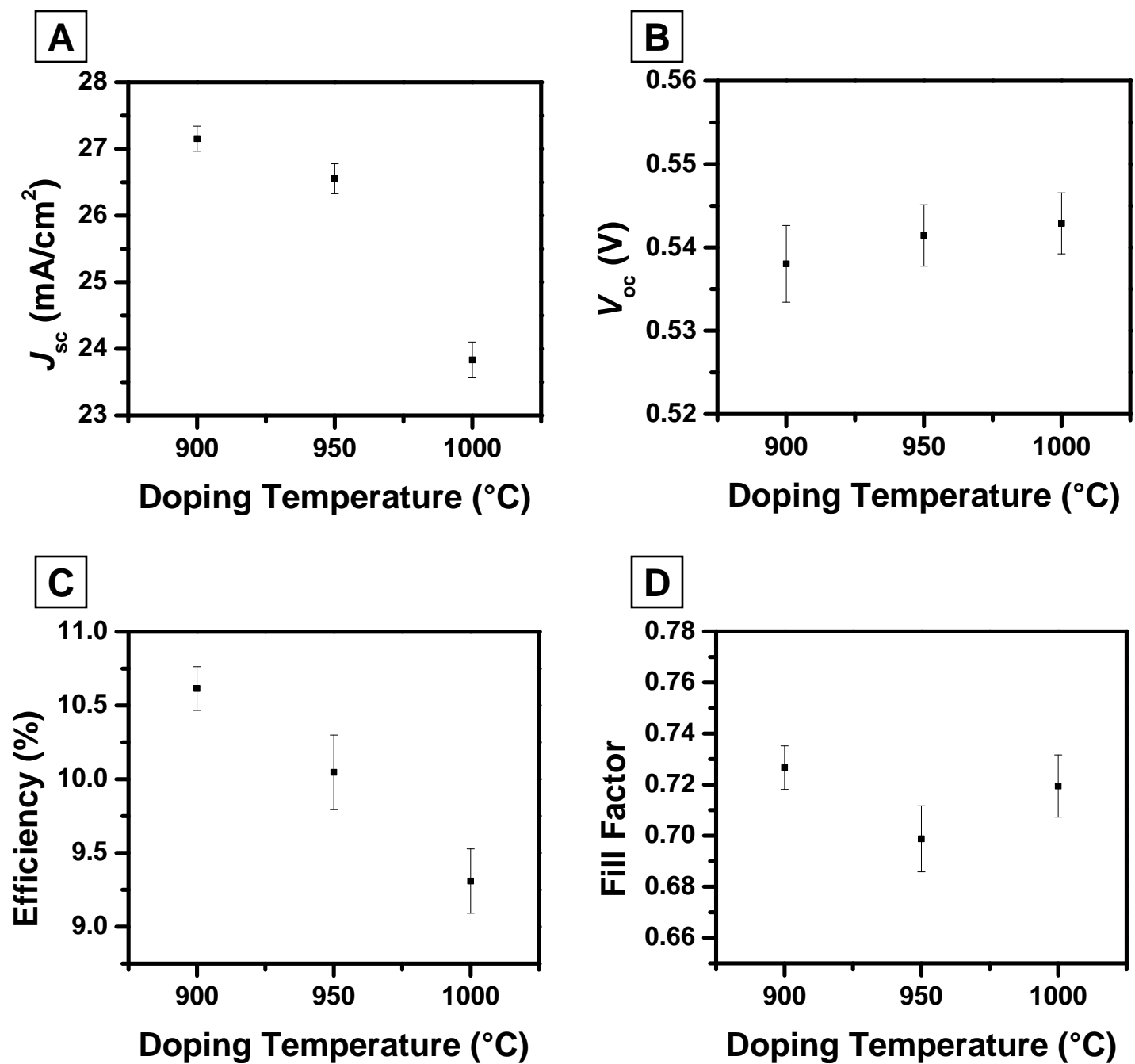


Figure S4

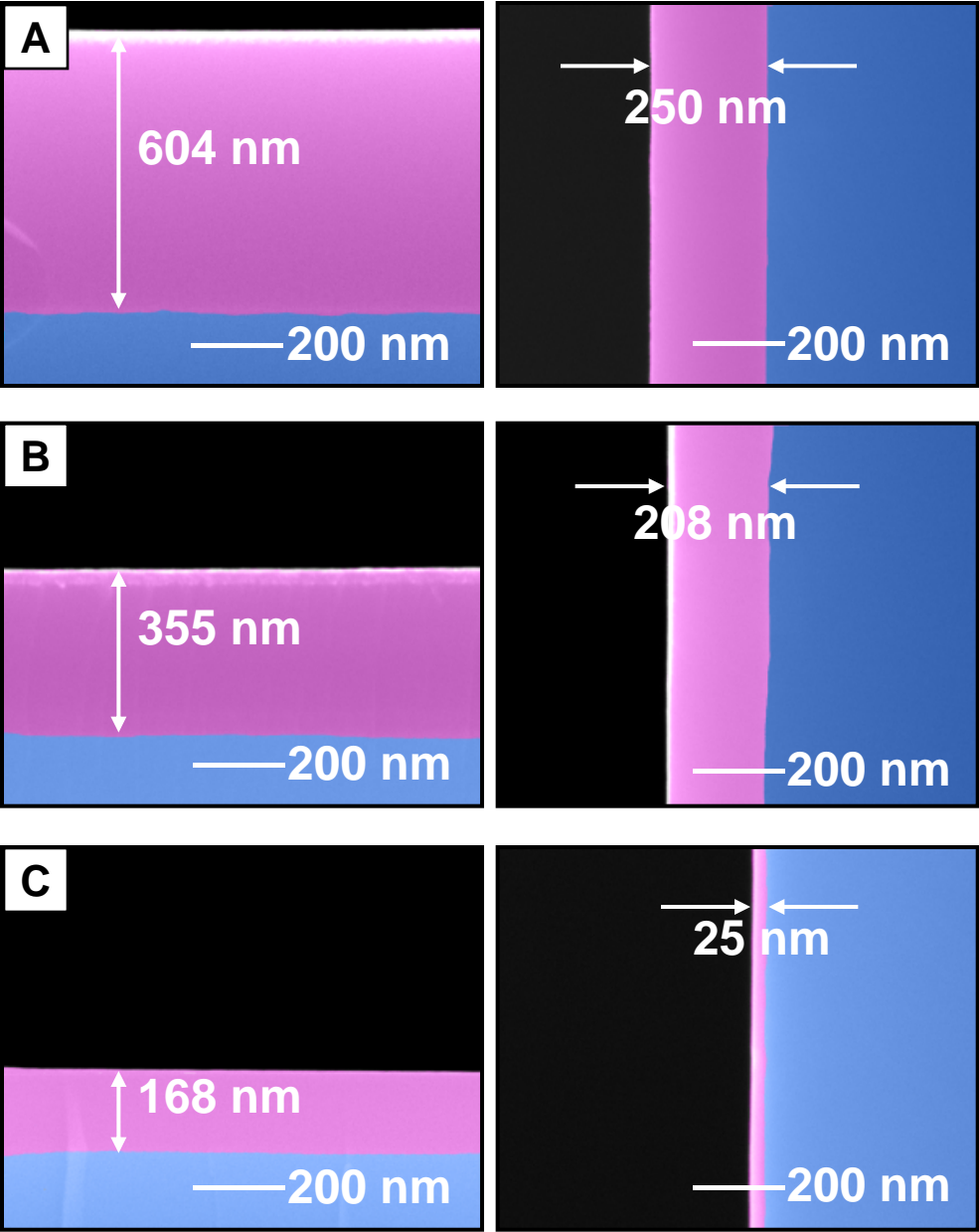


Figure S5

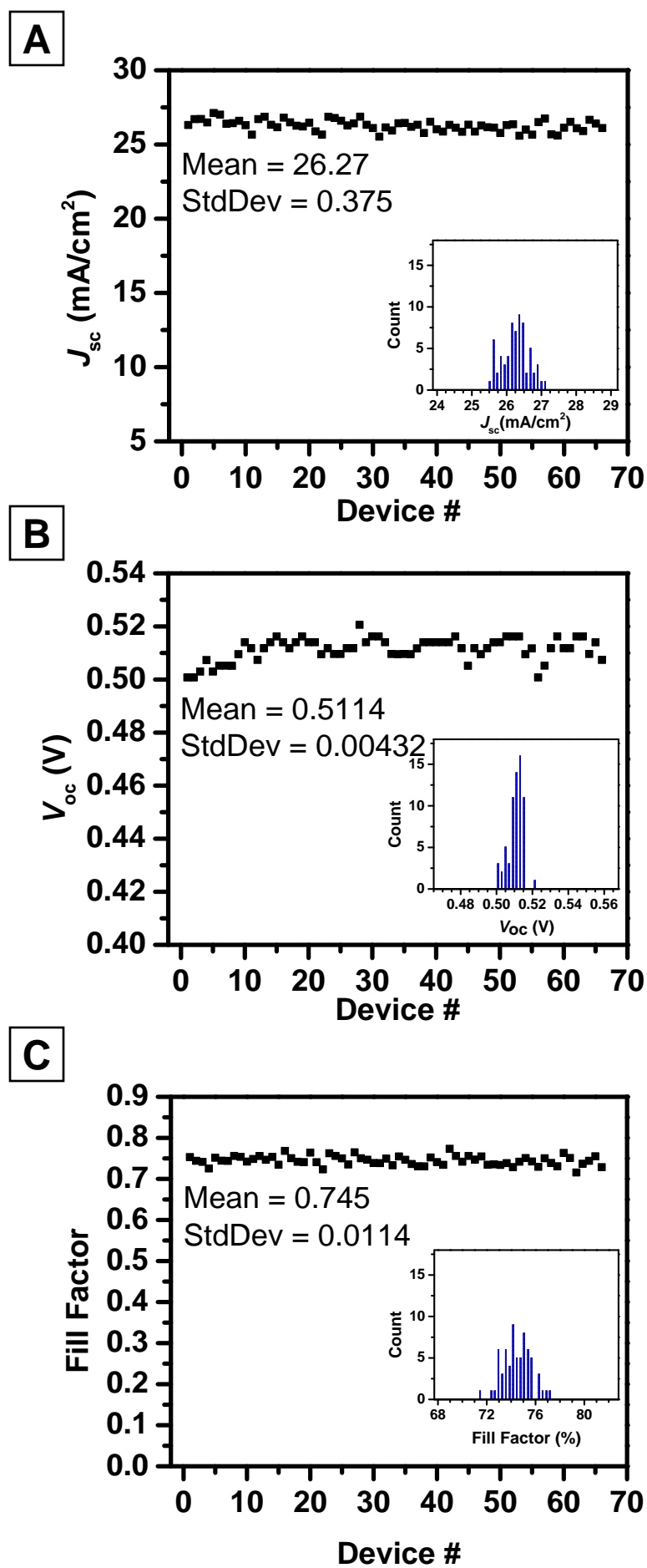


Figure S6

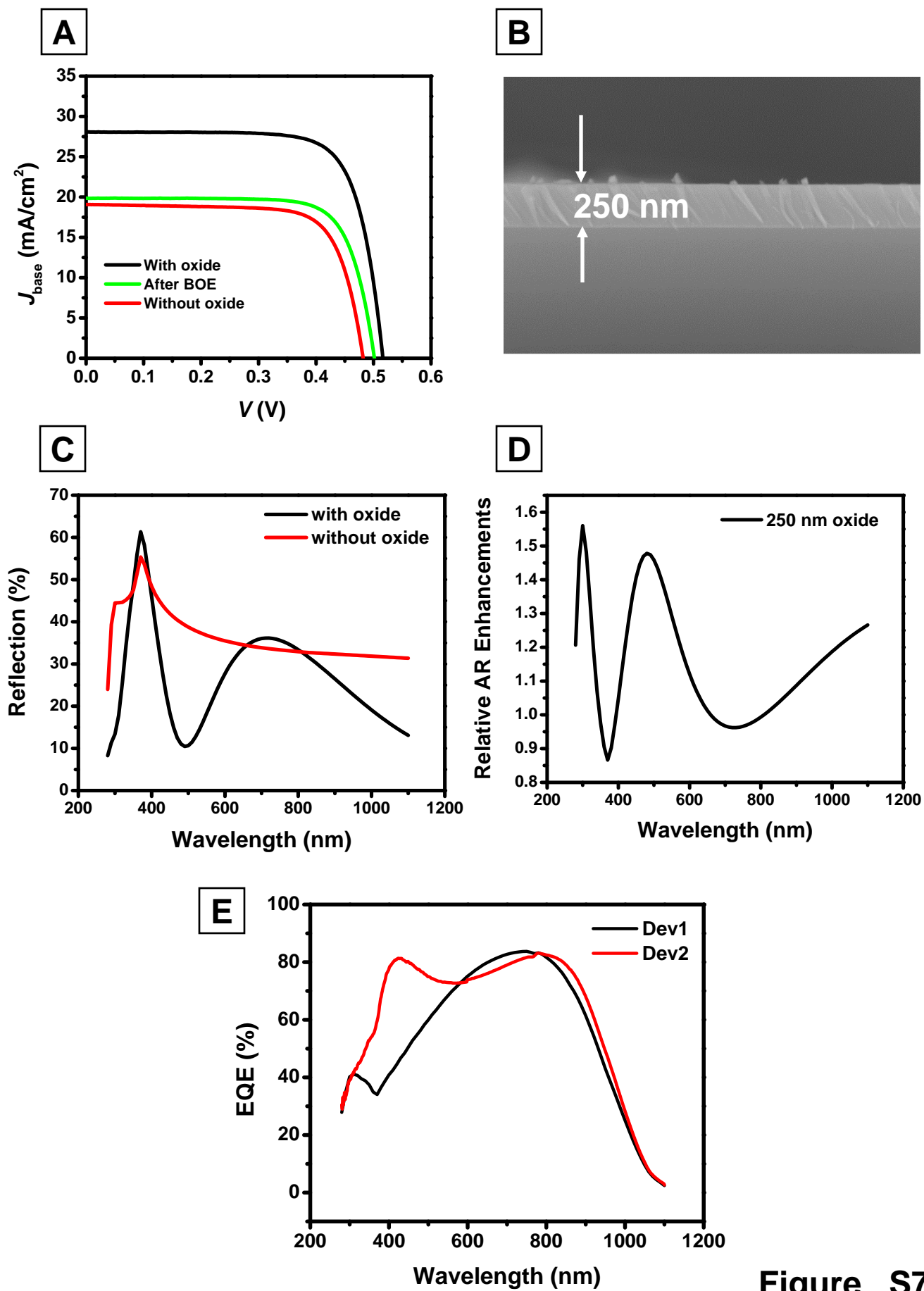


Figure S7

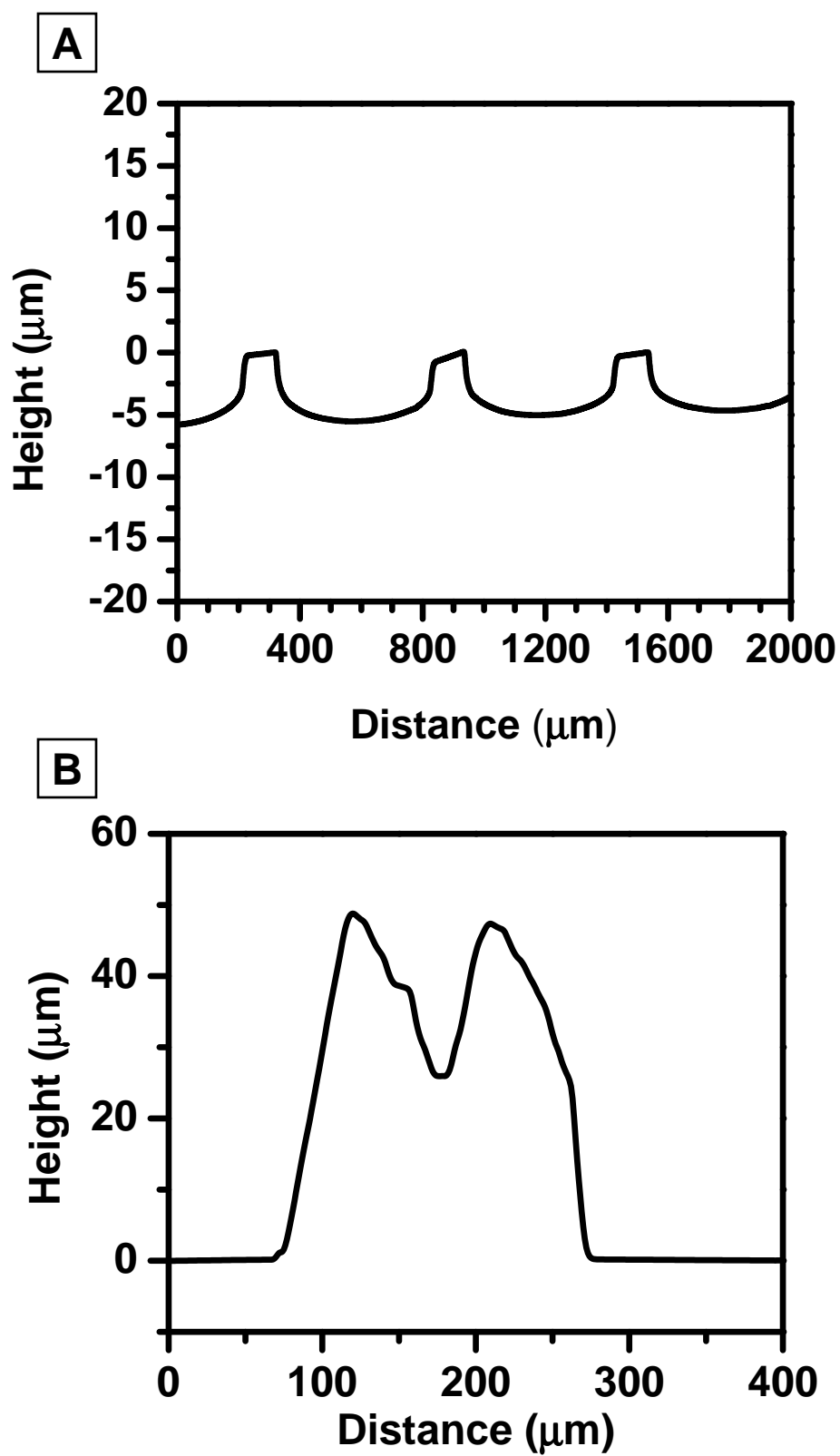


Figure S8

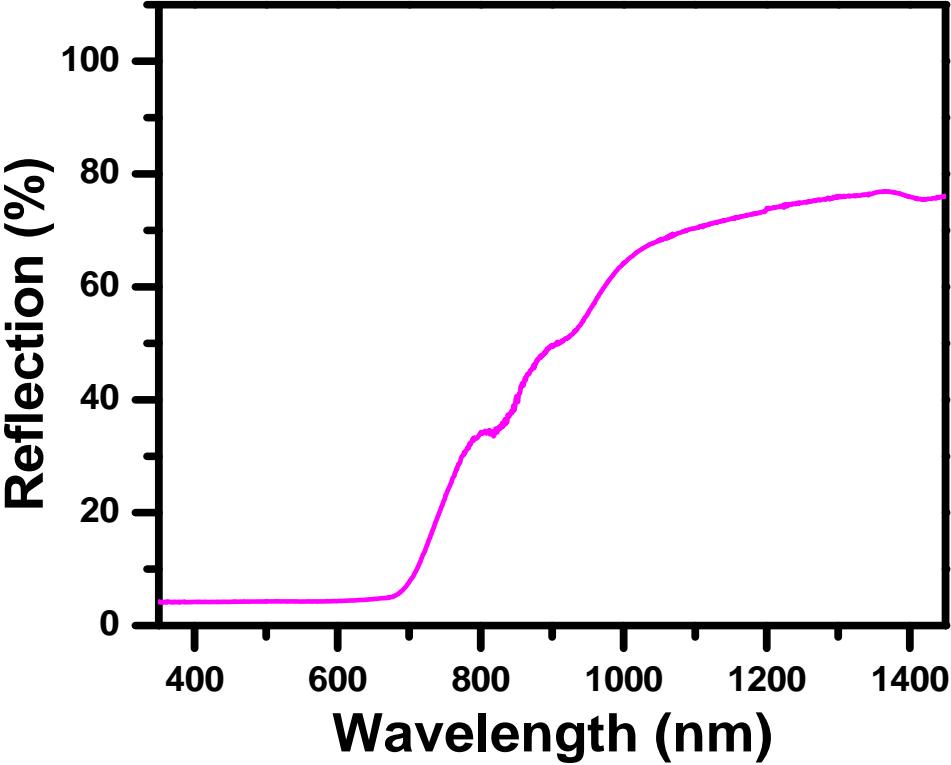


Figure S9